THE JOURNAL OF BIOLOGICAL CHEMISTRY
Vol. 277, No. 44, Issue of November 1, pp. 42325–42333, 2002

Printed in U.S.A.

Dual Recognition of the Bacterial Chemoreceptor by Chemotaxis-specific Domains of the CheR Methyltransferase*

Received for publication, February 28, 2002, and in revised form, July 2, 2002
Published, JBC Papers in Press, July 5, 2002, DOI 10.1074/jbc.M202001200

Daisuke Shiomi‡, Igor B. Zhulin§, Michio Homma‡, and Ikuro Kawagishi‡¶

From the ‡Division of Biological Science, Graduate School of Science, Nagoya University, Chikusa-ku, Nagoya 464-8602, Japan, and the §School of Biology, Georgia Institute of Technology, Biology Department, Atlanta, Georgia 30332-0230

Adaptation to persisting stimulation is required for highly sensitive detection of temporal changes of stimuli, and often involves covalent modification of receptors. Therefore, it is of vital importance to understand how a receptor and its cognate modifying enzyme(s) modulate each other through specific protein-protein interactions. In the chemotaxis of *Escherichia coli*, adaptation requires methylation of chemoreceptors (*e.g.* Tar) catalyzed by the CheR methyltransferase. CheR binds to the C-terminal NWETF sequence of a chemoreceptor that is distinct from the methylation sites. However, little is known about how CheR recognizes its methylation sites or how it is distributed in a cell. In this study, we used comparative genomics to demonstrate that the CheR chemotaxis methyltransferase contains three structurally and functionally distinct modules: (i) the catalytic domain common to a methyltransferase superfamily; (ii) the N-terminal domain; and (iii) the β-subdomain of the catalytic domain, both of which are found exclusively in chemotaxis methyltransferases. The only evolutionary conserved motif specific to CheR is the positively charged face of helix α2 in the N-terminal domain. The disulfide cross-linking analysis suggested that this face interacts with the methylation helix of Tar. We also demonstrated that CheR localizes to receptor clusters at cell poles via interaction of the β-subdomain with the NWETF sequence. Thus, the two chemotaxis-specific modules of CheR interact with distinct regions of the chemoreceptor for targeting to the receptor cluster and for recognition of the substrate sites, respectively.

In many sensory systems, transmembrane receptors recognize extracellular stimuli and transduce them into cytoplasmic signals to trigger defined physiological responses. These initial responses often diminish during persisting stimulation. The latter process, termed adaptation or desensitization, is essential for the detection of temporal changes of stimuli and/or the highly sensitive detection of stimuli over a comprehensive range. Covalent modifications of a receptor are often required for adaptation. In such cases, it is of vital importance to understand a regulated interplay between a receptor and modifying enzyme(s), including their mutual recognition and their subcellular localization, that assures spatially and temporally organized information processing.

Molecular mechanisms of adaptation have been well characterized in the chemotaxis of *Escherichia coli* and *Salmonella typhimurium* (1–6). The transmembrane chemoreceptors, also known as the methyl-accepting chemotaxis proteins (MCPs),[1] are methylated by the *S*-adenosylmethionine (AdoMet)-dependent methyltransferase (MTase) CheR and demethylated by the methylesterase CheB. In the resting state, an MCP is in equilibrium between methylation and demethylation. An attractant shifts the equilibrium toward methylation and a repellent toward demethylation. Each MCP has 4–5 glutamate residues located in two separate α helices (the first and second methylation helices (MH1 and MH2)) in the cytoplasmic domain (7, 8). CheR has to recognize these residues (*i.e.* the substrate sites), but this interaction between CheR and an MCP has not been detected to date probably because it is weak and/or transient.

In contrast, binding of CheR to the C-terminal pentapeptide sequence (NWETF) of the two high abundance receptors, the serine chemoreceptor Tsr and the aspartate chemoreceptor Tar, has been well characterized (9–12). However, the low abundance chemoreceptors (the ribose-galactose transducer Trg and the dipeptide transducer Tap) do not have the sequence, indicating that the binding of CheR to the NWETF sequence might not be essential for its catalytic activity itself.

The three-dimensional structure of CheR of *S. typhimurium* revealed that the monomeric protein consists of two domains (the N-terminal domain with no assigned function and the MTase domain) and one subdomain (the β-subdomain) (13). The co-crystal of CheR and the pentapeptide revealed that the β-subdomain binds to the NWETF sequence (11). Mutagenesis of the NWETF sequence of Tar demonstrated that it binds to CheR mainly through hydrophobic interaction (12). However, it is not clear how the CheR molecule is oriented when it binds to a chemoreceptor, nor how the NWETF sequence is oriented relative to the other part of the chemoreceptor molecule.

Recently, subcellular localization of some proteins involved in chemotactic signal transduction (MCPs and Che proteins) has been studied using immunoelectron and immunofluorescence microscopy and YFP fusion proteins (14–18). These studies demonstrated that MCPs cluster with the histidine kinase CheA and the adaptor protein CheW at cell poles. The localization and the clustering depend, at least to some extent, on CheA and CheW, but not on CheR or CheB. The localization and clustering of the chemotactic machinery at cell poles are proposed to be essential for amplification of input signals and

* This work was supported in part by grants-in-aid for scientific research from the Japan Society for the Promotion of Science (to D. S. and I. K.) and by start-up funds from Georgia Institute of Technology (to I. B. Z). The costs of publication of this article were defrayed in part by the payment of page charges. This article must therefore be hereby marked "*advertisement*" in accordance with 18 U.S.C. Section 1734 solely to indicate this fact.

¶ To whom correspondence should be addressed. Tel.: 81-52-789-2993; Fax: 81-52-789-3001; E-mail: i45406a@cc.nagoya-u.ac.jp.

[1] The abbreviations used are: MCP, methyl-accepting chemotaxis protein; AdoMet, *S*-adenosylmethionine; GFP, green fluorescent protein; MBP, maltose-binding protein; MH, methylation helix; MTase, methyltransferase.

for efficient methylation. The latter hypothesis assumes a high local concentration of CheR around the receptor/kinase cluster to provide a molecular basis of efficient methylation of both high abundance and low abundance receptors. Previous studies (10, 12, 19–21) suggest that the NWETF sequence may serve to concentrate CheR around MCPs, but no direct evidence has been obtained.

Moreover, the information about the structure-function relation of CheR was limited although the three-dimensional structure of *S. typhimurium* CheR has been determined in the absence and presence of the NWETF peptide (11, 13) and the mutagenesis of the cysteine residues of *S. typhimurium* CheR (22) was carried out. In this study, we took advantage of comparative genomic analysis to identify evolutionary conserved and therefore structurally and functionally important residues in the CheR protein family. Mutagenesis of some conserved residues in *E. coli* CheR demonstrated that some of them are functionally important. Characterization of GFP-CheR revealed that CheR localizes to cell poles through the interaction between its β-subdomain and the NWETF sequence of the chemoreceptor. Disulfide cross-linking assay was employed to examine the interaction between CheR and Tar and demonstrated that the positively charged residues in helix α2 of CheR are involved in the recognition of MH1. Thus, CheR interacts with the chemoreceptor through two distinct chemotaxis-specific modules to achieve efficient adaptation.

EXPERIMENTAL PROCEDURES

Data Base Searches and Protein Sequence Analysis—BLAST searches (23) of nonredundant and individual microbial genomes data bases at the National Center for Biotechnology Information (Bethesda, MD) were performed with default parameters. Position-specific iterative BLAST searches (23) were performed with defined parameters (BLOSUM62 matrix, an inclusion threshold of $E = 0.01$ and composition based statistics). Searches were iterated to convergence and repeated with all newly found homologues as queries. CheR and related sequences from unfinished microbial genomes were identified in tBLASTn searches at www.ncbi.nlm.nih.gov/cgi-bin/Entrez/genom_table_cgi followed by gene finding and translation using the FramePlot program at www.nih.go.jp/~jun/cgi-bin/frameplot.pl. Profile hidden-Markov-model searches against SMART (24) and Pfam (25) data bases were performed with default parameters. Multiple alignments were constructed using the ClustalX program (26). Visualization of the three-dimensional structure of CheR was achieved using a Swiss-PDB viewer (27).

Bacterial Strains and Plasmids—All strains used in this work are derivatives of *E. coli* K12. Strain RP437 is wild-type for chemotaxis (28). Strain RP4944 (Δ*cheR his pyrC46 thyA araD139* Δ*lac-U169 nalA rpsL thi*) lacks CheR,[2] and RP8691 (Δ*tsr-7021 zec*::Tn*10* Δ*cheR leuB6 his-4 metF159*(Am) *eda-50 rpsL163 thi-1 ara-14 lacY1 mtl-1 xyl-5 tonA31 tsx-78*) lacks CheR and Tsr (29). Strain HCB436 (Δ*tsr-7021* Δ(*tar-cheB)2234* Δ*trg-100 zbd*::Tn*5 thr leu his met rpsL136*) (30) lacks CheB and CheR as well as MCPs, and strain HCB1262 (Δ(*cheA-cheZ*)::*zeoR thr leu his met rpsL136*)[3] lacks all of the Che proteins involved in general chemotaxis as well as MCPs.

Plasmids used in this study are listed in Table I. Plasmid pTrcHisB (Invitrogen) carries the *trc* promoter, the $lacI^q$ and *bla* genes. Plasmid pBAD24 (31), which was provided by J. Beckwith, carries the *araBAD* promoter, the *araC* gene encoding the positive and negative regulator, and the *bla* gene. Plasmid pMAL-c2 (New England Biolabs) carries the mutant *malE* gene, which encodes the mature maltose-binding protein (MBP) without its leader sequence, under the control of the *tac* promoter, the $lacI^q$ gene, and the *bla* gene. Plasmid pACYC184 and its derivative pSU21 (32) carry the *cat* gene. The pSU21-based plasmid, pDS2 (12), carries the wild-type *cheR* gene. The pACYC184-based plasmid, pLC113 (33), which was provided by J. S. Parkinson, carries the wild-type *tar* gene under control of the *nahG* promoter. Plasmid pEGFP (CLONTECH) encodes the enhanced green fluorescent protein.

Site-directed mutagenesis of the *cheR* and *tar* genes was performed according to the two-step PCR method (34) using primers synthesized by Life Tech Oriental (Tokyo) and Pyrobest DNA polymerase (Takara Shuzo, Kyoto). For the tight regulation of CheR proteins (*i.e.* CheR, His_6-CheR, and GFP-CheR proteins), the coding regions were placed downstream of the *araBAD* promoter on vector pBAD24. For the expression of MBP-Tar, the 3′ region of *tar* (encoding the cytoplasmic domain, *i.e.* residues 215–553) was introduced into the vector pMAL-c2.

Swarm Assay of Chemotaxis—Swarm assays were performed essentially as described previously (10) using tryptone semisolid agar supplemented with appropriate antibiotics and, when necessary, with various concentrations of arabinose and fucose.

Analysis of Receptor Methylation by Immunoblotting—Receptor methylation was monitored by immunoblotting as described previously (10) with anti-Tsr serum (38), which cross-reacts with Tar, and alkaline phosphatase-conjugated anti-rabbit IgG (Vector Laboratories) as the first and the second antibodies (at the dilution of 1:3000).

Observation of Subcellular Localization of GFP-CheR—HCB436 cells carrying pLC113 encoding wild-type Tar, pLC113-W550Op encoding Tar-N*, or the vector pACYC184 were further transformed with pBR322-based plasmids encoding the GFP-CheR fusion proteins. Cells were grown in TG medium containing appropriate antibiotics and inducers with vigorous shaking at 30 °C, harvested at late exponential phase, washed twice with MLM (10 mM potassium phosphate buffer (pH 7.0), 0.1 mM EDTA, 10 mM DL-lactate, 0.1 mM methionine), and resuspended in MLM. A small aliquot of the cell suspension was spotted onto slide glasses coated with 0.5% agarose and was observed under a fluorescence microscope (Olympus, BX50). The images were recorded and processed by using a digital camera (Hamamatsu Photonics, C4742-95) and imaging software (Scanalytics, IP Lab version 3.2).

Disulfide Cross-linking Assay—HCB1262 cells expressing any of the His_6-tagged CheR proteins were suspended in 2 ml of lysis buffer (50 mM NaH_2PO_4 (pH 8.0), 300 mM NaCl, and 10 mM imidazole) containing 10 mM dithiothreitol, and sonicated in short pulses (10 s each) on ice. After low speed (17,000 × *g* at 4 °C for 10 min) and high speed (100,000 × *g* at 4 °C for 30 min) centrifugation, the resulting supernatant was applied to a nickel-nitrilotriacetic acid-agarose column (Qiagen). Each His_6-tagged CheR protein was eluted with 250 mM imidazole. HCB1262 cells expressing MBP-Tar-E308C were suspended in 2 ml of column buffer (20 mM Tris-HCl (pH 7.4), 200 mM NaCl, and 1 mM EDTA) containing 10 mM dithiothreitol, and sonicated in short pulses on ice. After low speed and high speed centrifugation, the supernatant was applied to the amylose column (New England BioLabs). MBP-Tar-E308C was eluted with 10 mM maltose. Each His_6-tagged CheR protein and MBP-Tar-E308C were mixed and incubated at 37 °C for 20 min in the presence or absence of 0.1 mM I_2. The mixture was divided into two aliquots, which were boiled at 100 °C for 3 min with or without 2-mercaptoethanol and were subjected to SDS-PAGE followed by immunoblotting with anti-CheR serum (12), at a dilution of 1:2000, or anti-MBP serum (New England BioLabs) at a dilution of 1:10000. The first antibodies were detected with horseradish peroxidase-conjugated anti-rabbit IgG (New England BioLabs) at the dilution of 1:3000 and with an ECL detection kit (Amersham Biosciences).

RESULTS

Comparative Protein Sequence Analysis of the CheR Protein—Initial analysis of the domain architecture of the CheR protein identified not only homologous CheR proteins from a variety of species, but also several types of multidomain proteins with a core domain corresponding to that of CheR. (Fig 1). Position-specific iterative BLAST searches with the N-terminal domain (residues 1–90) of *S. typhimurium* CheR (13) retrieved only corresponding domains from homologous CheR proteins from bacterial and archaeal species, indicating that this domain is present exclusively in chemotaxis-related MTases (Figs. 1 and 2*A*). Searches with the catalytic domain (residues 91–286) retrieved sequences of nonchemotactic AdoMet-dependent MTases, including DNA MTases and rRNA dimethyltransferases, from both prokaryotes and eukaryotes (Figs. 1 and 2*B*): hundreds of functionally divergent MTases were identified in the third and forth iterations with a high degree of statistical significance (expectation value E ranged from 10^{-4} to 10^{-8}).

Domain organization of all types of MTases retrieved during the data base searches is shown in Fig. 1. FrzF of *Myxococcus xanthus*, a known functional CheR homolog (39), contains sev-

[2] J. S. Parkinson, personal communication.
[3] H. C. Berg, personal communication.

TABLE I
Plasmids used in this study

Plasmid	Relevant phenotype	Vector	Source
pBAD24			(32)
pSU21			(33)
pDS2	CheR	pSU21	(12)
pDS80	CheR	pBAD24	This study
pDS81A	CheR-K46A	pBAD24	This study
pDS81E	CheR-K46E	pBAD24	This study
pDS82	CheR-V50A	pBAD24	This study
pDS83A	CheR-R53A	pBAD24	This study
pDS83E	CheR-R53E	pBAD24	This study
pDS84	CheR-L54A	pBAD24	This study
pDS85A	CheR-R57A	pBAD24	This study
pDS85E	CheR-R57E	pBAD24	This study
pDS86	CheR-R98A	pBAD24	This study
pDS87	CheR-D154A	pBAD24	This study
pDS88A	CheR-R187A	pBAD24	This study
pDS88E	CheR-R187E	pBAD24	This study
pDS89	CheR-H192A	pBAD24	This study
pDS90	CheR-R197A	pBAD24	This study
pDS91	CheR-H192A/R197A	pBAD24	This study
pDS92	CheR-C7S	pBAD24	This study
pDS93	CheR-C229S	pBAD24	This study
pDS94	CheR-C7S/C229S (CheR-CS)	pBAD24	This study
pDS200	His_6-CheR-CS	pBAD24	This study
pDS201	His_6-CheR-CS-K46C	pBAD24	This study
pDS202	His_6-CheR-CS-R53C	pBAD24	This study
pDS203	His_6-CheR-CS-L54C	pBAD24	This study
pDS204	His_6-CheR-CS-L55C	pBAD24	This study
pDS205	His_6-CheR-CS-R56C	pBAD24	This study
pDS206	His_6-CheR-CS-R57C	pBAD24	This study
pDS207	His_6-CheR-CS-L58C	pBAD24	This study
pDS208	His_6-CheR-CS-R59C	pBAD24	This study
pDS209	His_6-CheR-CS-S60C	pBAD24	This study
pDS210	His_6-CheR-CS-K46C/R53A	pBAD24	This study
pDS220	GFP	pBAD24	This study
pDS221	GFP-CheR	pBAD24	This study
pDS222	GFP-CheR-R53A	pBAD24	This study
pDS223	GFP-CheR-D154A	pBAD24	This study
pDS224	GFP-CheR-H192A/R197A	pBAD24	This study
pLC113	Tar	pACYC184	(31)
pDS1015	Tar-W550Op (Tar-N*)	pACYC184	This study
pDS850	MBP-Tar-EEEE-E308C	pMAL-c2	This study
pDS851	MBP-Tar-QQQQ-E308C	pMAL-c2	This study
pMAL-c2			New England Biolabs
pEGFP			Clontech
pTrcHisB			Invitrogen

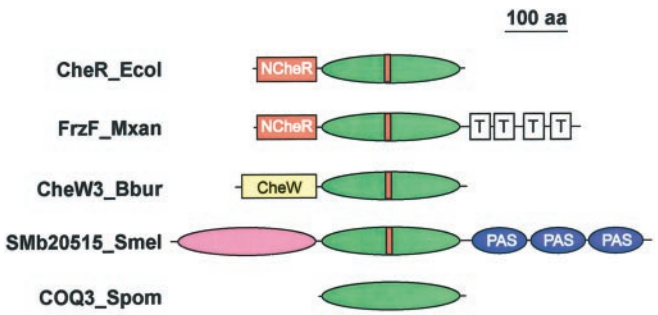

FIG. 1. **Domain architecture of CheR and related MTases.** Domain architecture of the MTase superfamily was determined by position-specific iterative BLAST and profile hidden-Markov-model based searches. Abbreviations: *NCheR*, the N-terminal domain found exclusively in chemotaxis MTases; *CheW*, a domain homologous to the CheW docking protein (43); *T*, the tetratrico peptide repeat (40); *PAS*, the PAS domain (42). *Green oval* depicts the MTase (catalytic) domain and the *purple oval* depicts the methylesterase (MEase (catalytic) domain. *Red rectangle* within the MTase domain corresponds to the β-subdomain of the CheR protein. Species abbreviations are the same as in a complete list of abbreviations shown in Fig. 2.

eral tetratrico peptide repeats in its C terminus. Tetratrico peptide repeats is thought to facilitate protein-protein interactions in various signal transduction proteins (40, 41). An unusual fusion protein containing catalytic domains of methylesterase and MTase as well as several PAS domains that may also facilitate protein-protein interactions (42) have been identified in several proteobacterial species, *e.g.* in *Sinorhizobium meliloti* (Fig. 1). Finally, a CheR-like protein from spirochetes lacks the N-terminal domain of a classical CheR, but instead has a CheW domain in its N terminus. The CheW protein is known to directly interact with MCPs (43).

Multiple sequence alignments of the N-terminal CheR-specific domains (Fig. 2*A*) revealed a conservation pattern centered on hydrophobic and turn-like residues comprising α-helices. Residue Gly-39, which determines a crucial turn following helix α1, is strictly conserved in all CheR homologs. The only two other positions where strict conservation occurs are positively charged residues Lys/Arg-46 and Arg-53 of helix α2. Such strict conservation of a positive charge across long evolutionary distances clearly indicates functional significance, especially for Arg-53.

Catalytic domains from most AdoMet-dependent MTases, including CheR, share a signature sequence (G/A)*X*(G/A/S)*X*G (Fig. 2*B*) involved in the binding of AdoMet (44). Interestingly, the β-subdomain is present in all CheR homologs and CheR-related proteins, such as PilK, FrzF, CheW3, and Smb20515, but is missing from all nonchemotactic single-domain MTases, such as COQ3 (Figs. 1 and 2*B*). This finding is consistent with the functional role of the β-subdomain, *i.e.* interaction with

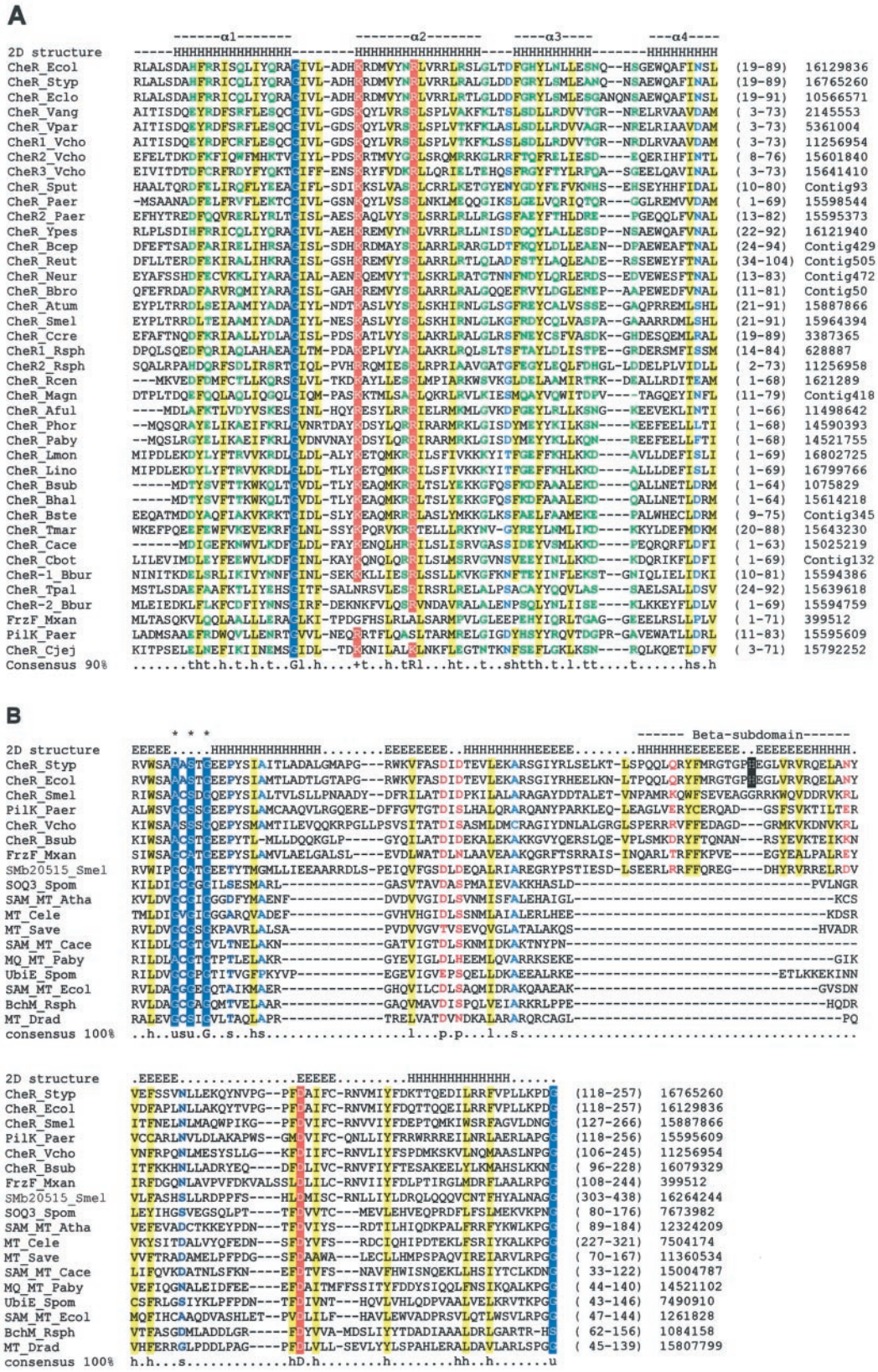

FIG. 2. **Multiple sequence alignments of the CheR-specific N-terminal domain (*A*) and a portion of the MTase (catalytic) domain including the β-subdomain (*B*).** Each sequence is identified by the NCBI gene identification number or by the sequencing center preliminary identification number (shown in the *last column*). The secondary structure (*E* for β-sheets and *H* for α-helices) shown *above* the alignments is based on the known three-dimensional structure of *S. typhimurium* CheR. The signature sequence involved in binding to AdoMet (44) is indicated by *three stars*, and a critical histidine residue (His-192) in the β-subdomain is highlighted in *black* (*panel B*). Conserved amino acid residues are

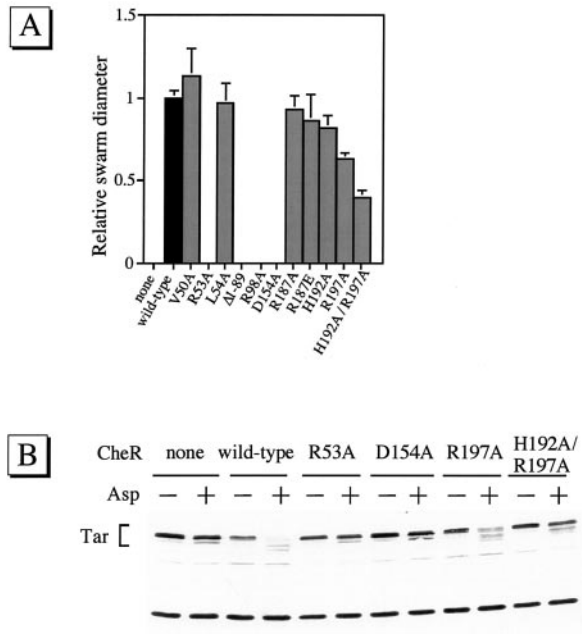

FIG. 3. *A*, swarming abilities of RP4944 cells expressing mutant CheR proteins. Aliquots (2 μl each) from fresh overnight cultures were spotted onto tryptone semi-solid agar (0.3%) supplemented with 50 μg/ml ampicillin, 0.1 mM arabinose (the inducer), and 0.1 mM fucose (the anti-inducer) and then the plate was incubated at 30 °C for 8 h. The swarm sizes of the three different colonies were measured for each mutant. The swarm diameter of cells carrying the vector pBAD24 (none) was subtracted from those of cells expressing each mutant CheR to obtain net swarm sizes. The relative swarm diameter was defined as the net swarm size normalized to that of cells expressing wild-type CheR. *B*, methylation levels of Tar co-expressed with each mutant CheR. Methylation of a receptor protein increases its mobility in SDS-PAGE and therefore can be detected by immunoblotting with anti-Tsr serum. The *lower band* is of an unidentified protein unrelated to Tar.

MCPs (11). CheR proteins from all chemotactic species retain the β-subdomain, although in many species all MCPs lack the NWETF-type sequence (data not shown). On the other hand, residues His-192 and Arg-197 of *S. typhimurium* CheR, which interact with the Trp residue of the NWETF pentapeptide (11), and residue Arg-187, which forms a salt bridge with the Glu residue of the pentapeptide (11), are absent from many CheR homologs (Fig. 2*B*).

Mutagenesis of Some Conserved Residues in E. coli CheR—We replaced some conserved residues of *E. coli* CheR by Ala or Glu. The resulting mutant proteins were expressed in strain RP4944 (ΔCheR) at levels similar to that of wild-type CheR (data not shown). Swarming abilities of these transformants were examined (Fig. 3*A*). RP4944 cells expressing either MTase domain mutants (R98A or D154A) failed to swarm, as expected. Among the β-subdomain mutations, H192A, R197A, and H192A/R197A significantly slowed the swarming rate. The defects in swarming were suppressed by the overproduction of these three mutant CheR proteins (data not shown). Thus, these three mutations may decrease the affinity of CheR for an MCP, consistent with the crystallographic study (11), which suggested that His-192 and Arg-197 interact with the Trp residue of the pentapeptide sequence. In contrast, R187A and R187E did not affect the ability of CheR to support swarming. Residue Arg-187 is suggested to form a salt bridge with the Glu residue of the NWETF sequence (11), but the E551A mutation of *E. coli* Tar had little effect on its methylation (12). Taken together, the salt bridge, if it is formed, may not play a critical role in the CheR function *in vivo*. Among the N-terminal domain mutations, V50A and L54A had no effect, but R53A and Δ1–89, in which residues 1–89 were deleted, impaired swarming, fully supporting predictions that resulted from our *in silico* analysis.

Next, we examined methylation levels of Tar in RP8691 (ΔTsr ΔCheR) cells expressing the mutant CheR proteins by immunoblotting with anti-Tsr, which cross-reacts with Tar (Fig. 3*B*). In RP8691 cells carrying the vector, methylation of Tar was hardly detected in the absence of aspartate but was slightly enhanced by the addition of aspartate, suggesting that the host strain has a residual activity of CheR. In the absence of aspartate, the methylation level of Tar in RP8691 cells expressing wild-type CheR was not much different from that of cells carrying the vector, but was greatly increased by the addition of aspartate, as expected. The MTase domain mutant (CheR-D154A) did not show any methylating activity, nor did the N-terminal domain mutant (CheR-R53A). Among the β-subdomain mutants, CheR-R197A and CheR-H192A/R197A were slightly impaired in the methylating activity. These results are consistent with those of the swarming assay (Fig. 3*A*).

Subcellular Localization of GFP-CheR—Previous studies demonstrated that MCPs together with CheA and CheW form clusters and localize to cell poles (14, 16, 17), and that CheY and CheZ also localize to cell poles in the presence of MCPs (18). CheR may also target to the receptor/kinase cluster. To visualize subcellular localization of CheR, we constructed a plasmid encoding GFP-CheR. Swarming ability of RP4944 cells expressing GFP-CheR was similar to those of cells expressing CheR (data not shown). We then examined subcellular localization of GFP-CheR in the presence of 1 mM arabinose (Fig. 4). With the lower concentrations of arabinose, the fluorescence bleached quickly, but arabinose concentration did not seem to affect localization of GFP-CheR (data not shown). In HCB436 (ΔMCPs ΔCheR ΔCheB) cells, GFP-CheR localized to cell poles in the presence of wild-type Tar, but not in the presence of the mutant Tar protein lacking the C-terminal NWETF sequence (Fig. 4, *left panels*). These results demonstrate that CheR is targeted to the MCP cluster through its binding to the NWETF sequence.

We next examined whether mutations in the CheR part of GFP-CheR affect its localization. The three severe mutations characterized above (R53A, D154A, and H192A/R197A), each representing one of the three domains, were tested. GFP-CheR with the D154A mutation (in the catalytic domain) localized to cell poles (Fig. 4, *right middle panel*) although the D154A mutation impairs the MTase activity (see Fig. 3, *A* and *B*).

colored according to 90 (*A*) or 100% (*B*) consensus (shown below alignments): polar (*p*, KRHEDQNST) in *red*; hydrophobic (*h*, LIVMYFW) and the aliphatic subset (*l*, ILV) with *yellow background*; turn-like (*t,* ACDEGHKNQRST) in *green*; small (*s,* ACDGNPSTV) in *blue*; tiny (*u*, AGS) in *white* with *blue background*; charged (*c*, DEHKR) and the positively charged subset of these (+, HKR) in *white* with *red background*. The species abbreviations are: *Aful*, *Archaeoglobus fulgidis*; *Atha*, *Arabidopsis thaliana*; *Atum*, *Agrobacterium tumefaciens*; *Bbro*, *Bordetella bronchiseptica*; *Bbur*, *Borrelia burgdorferi*; *Bcep*, *Burkholderia cepacia*; *Bhal*, *Bacillus halodurans*; *Bste*, *Bacillus stearothermophilus*; *Bsub*, *B. subtilis*; *Cace*, *Clostridium acetobutylicum*; *Cbot*, *Clostridium botulinum*; *Ccre*, *Caulobacter crescentus*; *Cele*, *Caenorhabditis elegans*; *Cjej*, *C. jejuni*; *Drad*, *Deinococcus radiodurans*; *Ecol*, *E. coli*; *Eclo*, *Enterobacter cloaceae*; *Lino*, *Listeria innocua*; *Lmon*, *Listeria monocytogenes*; *Magn*, *Magnetococcus* sp.; *Mxan*, *M. xanthus*; *Neur*, *Nitrosomonas europeae*; *Paby*, *Pyrococcus abyssi*; *Paer*, *Pseudomonas aeruginosa*; *Phor*, *Pyrococcus horikoshii*; *Reut*, *Ralstonia eutropha*; *Rcen*, *Rhodospirillum centenum*; *Rsph*, *Rhodobacter sphaeroides*; *Save*, *Streptomyces avermitilis*; *Smel*, *S. meliloti*; *Spom*, *Schizosaccharomyces pombe*; *Sput*, *Shewanella putrefaciens*; *Styp*, *Salmonella enterica* serovar *Typhimurium*; *Tmar*, *Thermotoga maritima*; *Tpal*, *Treponema pallidum*; *Vang*, *Vibrio anguillarum*; *Vcho*, *V. cholerae*; *Vpar*, *Vibrio parahemeolyticus*; *Ypes*, *Yersinia pestis*.

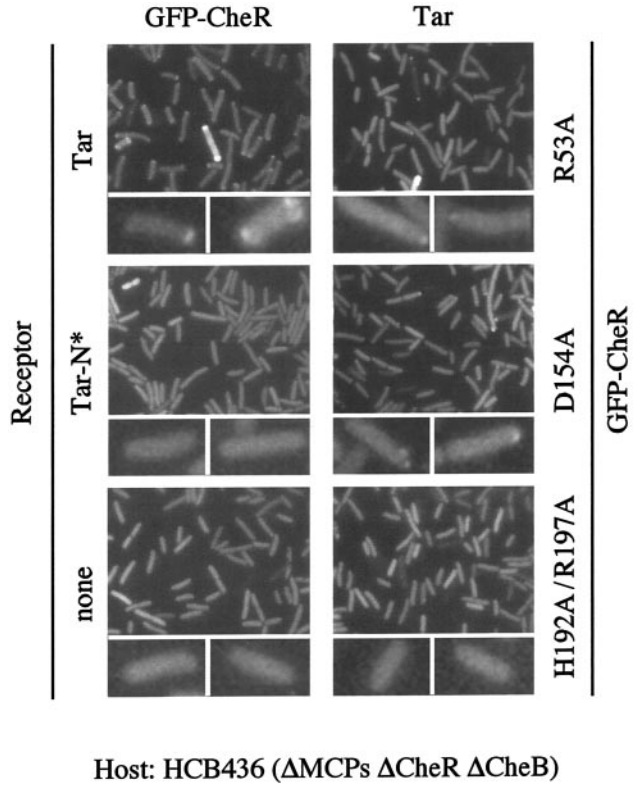

FIG. 4. **Subcellular localization of the wild-type and mutant versions of GFP-CheR.** The fusion proteins were expressed in HCB436 cells carrying the vector plasmid (*none*) or the plasmid encoding wild-type (NWETF) or the truncated (*N**) Tar protein. Sodium salicylate (0.1 μM) and arabinose (1 mM) were added to induce the expression of Tar and GFP-CheR, respectively. The images are shown for cells expressing wild-type GFP-CheR in the presence of wild-type Tar (*Tar*) or Tar-W550Op (*Tar-N**) and in the absence of Tar (*none*) or a mutant version of GFP-CheR with the R53A mutation (the N-terminal domain), the D154A mutation (the catalytic domain), or the H192A/R197A mutations (the β-subdomain) in the presence of wild-type Tar.

GFP-CheR with the H192A/R197A mutation (in the β-subdomain) did not localize to cell poles (Fig. 4, *right lower panel*), supporting the previous conclusion that the mutation may decrease the affinity of CheR for the NWETF sequence. Interestingly, GFP-CheR with the R53A mutation (in the N-terminal domain) localized to cell poles (Fig. 4, *right upper panel*), although the mutation severely impaired the CheR activity (Fig. 3, *A* and *B*). These results suggest that the targeting of CheR to cell poles does not depend on the MTase activity and the function of the N-terminal domain of CheR, but depends primarily on the binding of the β-subdomain of CheR to the C-terminal NWETF sequence of high abundance MCPs.

Mutagenesis of Positively Charged Residues in Helix α2 of CheR—The R53A mutation severely impaired the CheR function without affecting its subcellular localization. However, cells expressing CheR-R53A produced larger swarm with increasing levels of expression (Table II), raising a possibility that residue Arg-53 is not directly involved in the catalytic activity. Helix α2 of CheR that contains Arg-53 has a face with many positively charged residues (Fig. 5, *left*) that constitutes a part of the "receptor interaction opening" together with the active center and the β-subdomain (13). On the other hand, the first methylation helix (MH1) of Tar that contains three of the four methylation sites has many residues with negatively charged or polar side chains (Fig. 5, *right*). Therefore, it is reasonable to speculate that the positively charged face of helix α2 may interact with the negatively charged face of MH1. To examine this possibility, we substituted Ala or Glu for some of the positively charged residues in helix α2 of CheR (K46A/E, R53A/E, and R57A/E).

TABLE II
Relative swarm diameter of RP4944 (ΔCheR) cells expressing each mutant CheR protein with an Ala or Glu substitution in helix α2

Swarming was examined with tryptone semi-solid agar (0.3%) supplemented with 50 μg/ml Ap and the indicated concentrations of arabinose (ara) and fucose (fuc). The relative swarm diameter was normalized to that of cells expressing wild-type CheR in the presence of 0.1 mM arabinose and 0.1 mM fucose.

Mutant	[Ara], [Fuc] (mM)				
	0, 0	0.1, 0.1	1, 0	5, 0	10, 0
None	0	0	0	0	0
WT	0	1.00	0.94	0.22	0.18
K46A	0	0.16	0.73	0.64	0.52
K46E	0	0	0	0	0
R53A	0	0	0.24	0.59	0.54
R53E	0	0	0	0	0
R57A	0	1.18	1.33	1.50	1.35
R57E	0	1.18	1.33	1.27	1.20

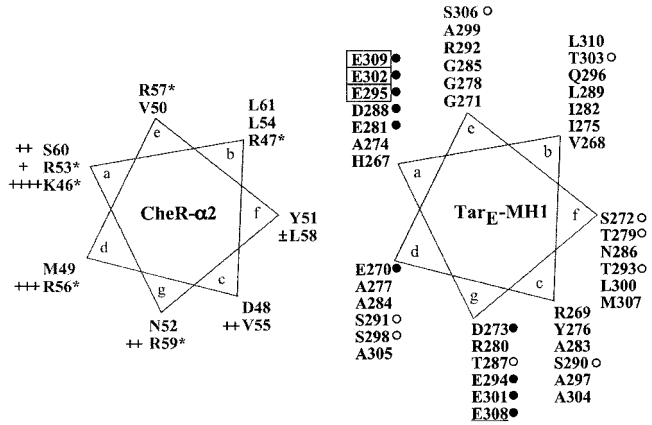

FIG. 5. **Helical wheel presentations of helix α2 of CheR (*left*) and the first methylation helix (*MH1*) of Tar (*right*).** Positively charged residues of CheR and the methylation sites of Tar are highlighted by *asterisks* and *boxes*, respectively. Residues with negatively charged and polar side chains of Tar are indicated with *closed* and *open circles*, respectively. Residue Glu-308, which was replaced by Cys, is *underlined*. The relative efficiency of cross-linking of the Cys-replaced CheR proteins with Tar is indicated with +. The cross-linking at L58C was only barely detectable (±).

Swarming abilities of RP4944 cells (ΔCheR) expressing the mutant CheR proteins were examined (Table II). Expression of wild-type CheR with 0.1 mM arabinose and 0.1 mM fucose resulted in the largest swarm ring. Overproduction of CheR impaired swarming presumably because overmethylation of MCPs caused tumbling-biased swimming and/or the titration of AdoMet by excess CheR impaired cell growth. Cells expressing CheR-K46A or R53A required higher concentrations of arabinose for swarming than cells expressing wild-type CheR. As the concentration of arabinose increased, the former cells swarmed faster. However, cells expressing CheR-K46E or R53E failed to swarm even in the presence of higher concentrations of arabinose. Thus, a Glu substitution seems to be more severe than an Ala substitution. Overproduction of CheR-R57A or R57E allowed the cells' swarming presumably because these proteins have weak activities or are unstable. These results suggest that the positive charges of helix α2 are important for the CheR function. Especially, Arg-53 seems to be critical, which is consistent with the results described above (Fig. 3).

Disulfide Cross-linking between CheR and MH1 of Tar—To detect directly the interaction between CheR and MH1 of Tar

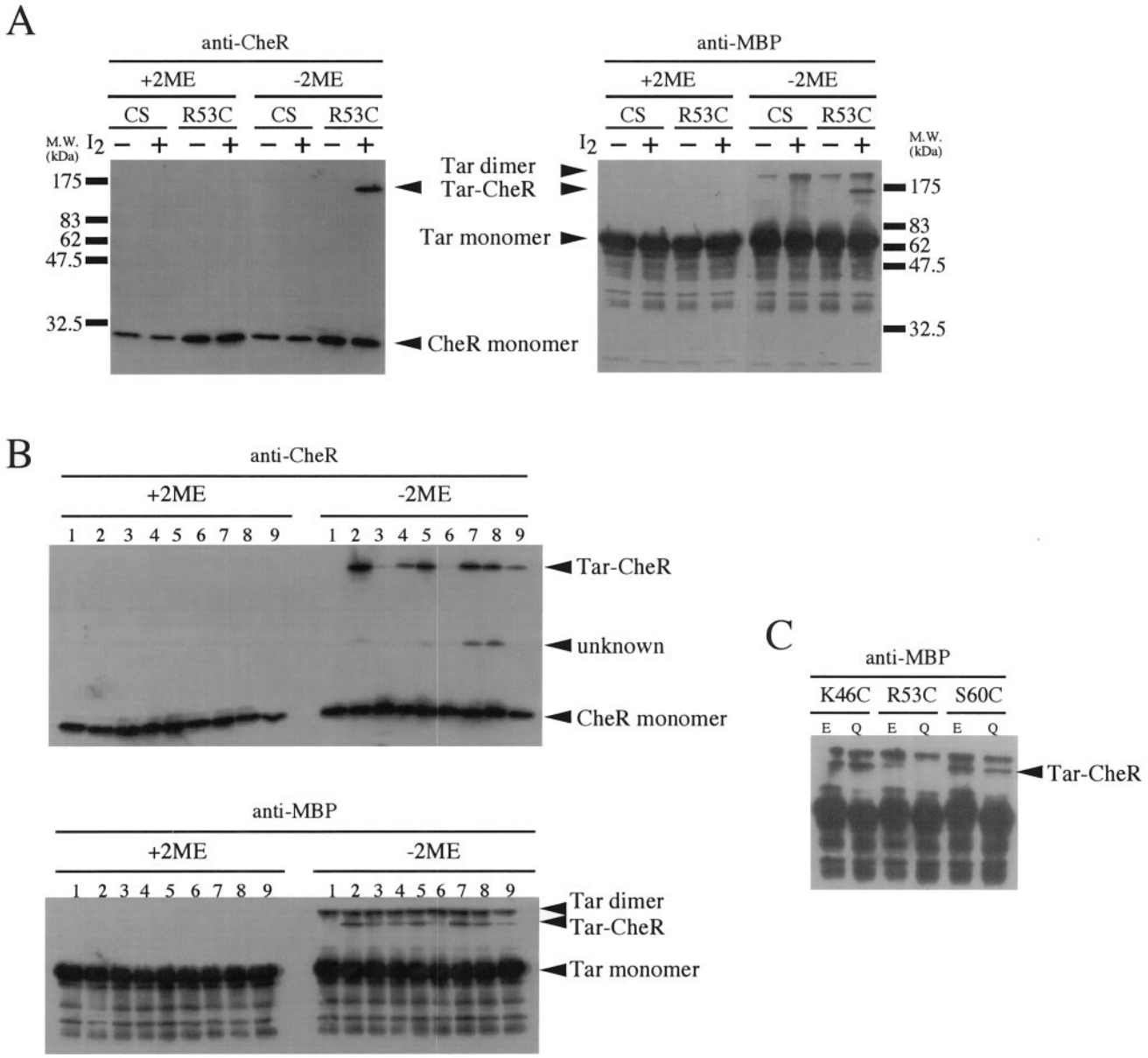

FIG. 6. **Disulfide cross-linking between CheR and Tar.** *A*, disulfide cross-linking between His_6-CheR-CS-R53C (lanes labeled with *R53C*) and MBP-Tar-EEEE-E308C with (lanes labeled with +) or without (lanes labeled with −) an oxidant (0.1 mM I_2). The Cys-less parental protein His_6-CheR-CS (lanes labeled with *CS*) was also tested as a control. *B*, disulfide cross-linking between the Cys-replaced derivatives of His_6-CheR-CS-CheR and MBP-Tar-EEEE-E308C. *Lane 1*, His_6-CheR-CS; *lane 2*, -K46C; *lane 3*, -R53C; *lane 4*, -V55C; *lane 5*, -R56C; *lane 6*, -L58C; *lane 7*, -R59C; *lane 8*, -S60C; *lane 9*, -K46C/R53A. *C*, effect of amidation of Tar on its interaction with CheR. The K46C, R53C, or S60C derivatives of His_6-CheR-CS were mixed with the EEEE (lanes labeled with *E*) or QQQQ (lanes labeled with *Q*) version of MBP-Tar-E308C. The samples were subjected to SDS-PAGE followed by immunoblotting with anti-CheR or anti-MBP serum as indicated.

that had been eluded from conventional biochemical assays, we employed a disulfide cross-linking assay. Wild-type CheR has two Cys residues (Cys-7 and Cys-229), but consistent with previous reports (22, 45), the substitution of Ser (C7S/C229S) had little effect on CheR function (data not shown). Cys-scanning mutagenesis was carried out for residues (Lys-46 and Arg-53 through Ser-60) in helix α2 of His_6-tagged Cys-less CheR (named His_6-CheR-CS). All of the resulting proteins were functional, but the L54C and R57C versions were not used in the following assay because of their low yields (data not shown).

Residue Glu-308 (underlined) of *E. coli* Tar lies in the consensus sequence around methylation sites (bold) ((E/Q)(**E/Q**)*XX*A(S/T)*X*) (46). This position was used as a target for cross-linking with CheR. A cytoplasmic fragment (residues 215–553) of the deamidated (EEEE) or the amidated (QQQQ) derivative of Tar-E308C was fused to the cytoplasmic version of the maltose-binding protein (named MBP-Tar-EEEE(or QQQQ)-E308C). Gln residues are known to mimic methylated Glu residues. RP437 (wild type for chemotaxis) cells expressing each MBP-Tar protein failed to swarm (data not shown), a dominant negative effect that suggests that Tar fragments are correctly folded to interact with some Che proteins.

We first identified the Tar-CheR cross-linked product. MBP-Tar-EEEE-E308C (about 79 kDa) was mixed with His_6-CheR-CS-R53C (about 34 kDa) in the presence of 0.1 mM I_2 (an oxidant) and detected by immunoblotting with anti-CheR and anti-MBP sera (Fig. 6*A*). The R53C protein, but not its Cys-less parental protein, gave a Tar-CheR cross-linked product with an apparent molecular mass a little higher than expected (about

113 kDa) but lower than that of the cross-linked dimer of MBP-Tar-EEEE-E308C (about 158 kDa). These cross-linked products were not detected in the presence of 2-mercaptoethanol.

MBP-Tar-EEEE-E308C was then mixed with each His_6-CheR derivative, and incubated at 37 °C for 20 min without addition of any oxidant (Fig. 6*B*). The K46C protein was most efficiently cross-linked to Tar (*lane 2*). The cross-linking of the L58C protein to Tar was only barely detectable and the V55C protein was much less effectively cross-linked to Tar than the K46C, R56C, R59C, and S60C proteins (*lanes 2* and *4–8*). The R53C protein was not effectively cross-linked to Tar (*lane 3*) presumably because Arg-53 is particularly important to recognize MH1. Indeed, the introduction of the R53A mutation into the K46C protein reduced the efficiency of cross-linking (compare *lanes 2* and *9*). These results suggest that the Cys residues in the positively charged face of α2 are more efficient for cross-linking to Tar than those in the opposite face and that the cross-linking reflects the ability of CheR to recognize MH1.

We also examined the effect of amidation of Tar on cross-linking with CheR. The His_6-CheR-CS proteins with K46C, R53C, or S60C were mixed with the EEEE or QQQQ version of MBP-Tar-E308C (Fig. 6*C*). The K46C protein was effectively cross-linked to MBP-Tar-E308C regardless of its amidation state. However, the R53C and S60C proteins were less effectively cross-linked to the amidated (QQQQ) fragment than to the deamidated (EEEE) one. This result reinforces the electrostatic nature of the interaction between MHs of MCPs and helix α2 of CheR.

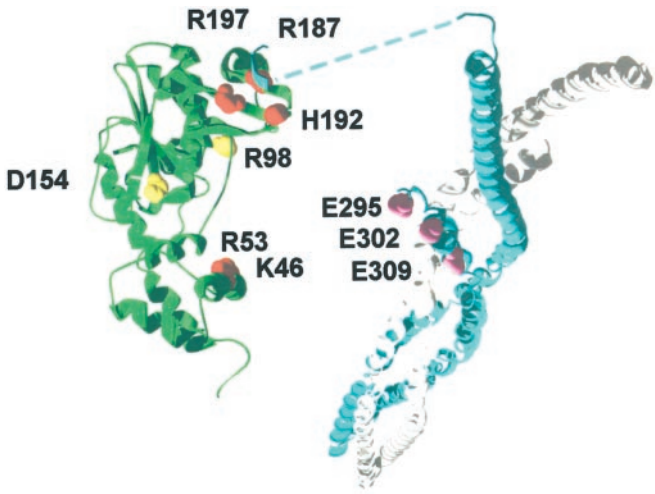

FIG. 7. **Two modes of interaction between CheR (*left*) and MCP (*right*).** The β-subdomain and the α2 helix of CheR interact with the C-terminal pentapeptide (NWETF) sequence and the MHs, respectively. The CheR structure (*green*) determined in the presence of the pentapeptide (*blue*) (11) is shown with the crystal structure of the cytoplasmic fragment of Tsr (8) by placing the α2 helix of CheR to face the first three methylation sites (*violet*) of one subunit (*blue*) of the Tsr dimer. The other subunit of Tsr is shown in *gray*. The NWETF sequence is tentatively connected to the main part of the cytoplasmic domain with a *broken line*, although it is not clear whether CheR can bind simultaneously to these two parts of the MCP. CheR residues involved in receptor recognition and catalysis are shown in *red* and *yellow*, respectively.

DISCUSSION

In this study, we examined how the MTase CheR interacts with its substrate, *i.e.* the chemoreceptor (MCP). More specifically, we asked how CheR is targeted to the receptor/kinase clusters at cell poles and how CheR recognizes the methylation sites of the chemoreceptor. We found that these two processes result from the distinct functions of CheR that reside in its two distinct domains.

Comparative protein sequence analysis of CheR homologs and related proteins revealed that all of the CheR proteins have two domains and one subdomain: the CheR-specific N-terminal domain, the catalytic domain, and the β-subdomain. This organization is consistent with the crystallography of *S. typhimurium* CheR, suggesting that all of the CheR proteins share a common three-dimensional structure. It is also possible that they share common basic mechanisms for catalysis and substrate recognition. However, MCPs of many bacteria lack the C-terminal NWETF-type sequence that serves as a primary binding site of CheR in *E. coli* and *S. typhimurium* although all of the CheR proteins have the β-subdomain, which binds to the NWETF sequence in the case of *S. typhimurium* and *E. coli* CheR (Ref. 11 and this study). The β-subdomain can be divided into two groups (11) (Fig. 2*B*): longer β-loops (*e.g. E. coli*, *S. typhimurium*, and *S. meliloti*) and shorter β-loops (*e.g. Vibrio cholerae* and *Bacillus subtilis*). The CheR proteins of the bacteria whose MCPs contain the C-terminal NWETF-like motif belong to the former group. This difference in the length of the β-loop might reflect the differences in the mode of receptor recognition by CheR.

In contrast to the recognition of the C-terminal tail of MCPs, little was known about the recognition of the methylation sites of MCPs by CheR. X-ray crystallography raised a possibility that the positively charged face of helix α2 of CheR might be involved in the interaction with MCPs (13). However, such an interaction had not been detected biochemically. Here, the mutagenesis and the disulfide cross-linking analyses indicated that the positively charged face in helix α2 of CheR is involved in the recognition of MH1 of Tar. This is the first direct demonstration of the interaction between CheR and a methylation helix of any MCP. Among the residues tested, Arg-53 seems to be the most important residue for the recognition of MH1. This residue is strictly conserved among all of the CheR proteins except for the *Campylobacter jejuni* homolog, in which the corresponding residue is Lys.

Thus, effective methylation requires two types of interaction between CheR and MCPs: one between the β-subdomain and the NWETF sequence (for the targeting of CheR to cell poles) and the other between the positively charged face in helix α2 and the negatively charged face of an MH (for the recognition of substrate sites) (Fig. 7). An *E. coli* cell expresses some 5,000 monomers of MCPs and only several hundred molecules of CheR (47). Therefore, the targeting of CheR to the C-terminal tail of MCPs may be required to concentrate CheR molecules around receptor/kinase clusters at cell poles. Increased probability of CheR to collide with MCP molecules may then allow it to interact with the negatively charged face of an MH. This interaction between helix α2 and an MH is predicted to be weak and/or transient. CheR might slide on the negatively charged face of MH1, which contains three methylation sites with intervals of two turns of the helix, to monitor the methylation sites.

It is still unknown how CheR is oriented when it binds to an MCP. The binding of the NWETF sequence to the β-subdomain was visualized by x-ray crystallography (11). However, it is unclear how the rest of the MCP molecule is oriented and whether CheR can catalyze methylation of an MCP molecule while it is anchored to the C-terminal tail of the same molecule or the partner subunit of the same dimer. It was also suggested that CheR can catalyze methylation of a neighboring MCP molecule within an MCP cluster (19, 20). This interdimer methylation explains why a low abundance MCP can be methylated efficiently in the presence of a high abundance MCP (48). Again, it is not clear whether this can be achieved without dissociation of CheR from the NWETF sequence. In any case, the

simultaneous anchoring and catalysis would require large flexibility of the MCP molecule. Because the affinity of CheR for the pentapeptide is not very high, it is also possible that CheR is dissociated from the NWETF sequence during catalysis.

We also examined subcellular localization of CheR. GFP-CheR localized to cell poles only in the presence of an MCP with the NWETF sequence. The mutagenesis of the CheR part suggested that the targeting of CheR to cell poles depends primarily on the interaction between CheR and the NWETF sequence. These results are consistent with the hypothesis that the NWETF sequence serves to concentrate CheR around MCPs at cell poles.

It should be noted that the abilities of the wild-type and mutant versions of GFP-CheR to localize to cell poles (Fig. 4, *right panels*) appeared to vary: wild-type > R53A > D154A. In the experimental conditions applied, the GFP-CheR proteins were mildly overproduced relative to chromosome-encoded CheR. Therefore, the methylation level of Tar would be different from one strain to another. This may suggest two possibilities: the methylation levels of MCPs might affect the subcellular localization of: (i) CheR and/or (ii) MCPs themselves. The high abundance MCPs (Tar and Tsr) localize to cell poles and form clusters with CheA and CheW, whereas the low abundance MCPs (Tap and Trg) also localize to cell poles but do not form a cluster (16). The latter receptors are poor substrates for CheR because they lack the C-terminal NWETF sequence. Taken together, it is possible that the methylation levels of MCPs would be critical for their clustering at cell poles. However, the polar localization of the high abundance MCPs does not seem to require CheR and CheB (15). Further analyses are required to clarify this issue.

The Cys-substituted CheR proteins were more effectively cross-linked to Tar-EEEE than to Tar-QQQQ. This may result from the electrostatic nature of the interaction between MHs of MCPs and helix α2 of CheR. It is also possible that receptor amidation (and hence methylation) alters the conformation of the MHs to reduce its affinity to helix α2 of CheR. In any case, this finding is consistent with the notion that upon methylation, an MCP becomes a poorer substrate of CheR.

CheB also binds to the C-terminal NWETF sequence of MCPs (49, 50) and has to recognize MHs of MCPs. However, CheB may be different from CheR in these respects. The affinity of CheB for the pentapeptide is much lower than that of CheR and the cellular concentration of CheB is much higher than that of CheR. Therefore, it is hard to imagine that the NWETF sequence serves to recruit CheB around MCPs. As for the substrate recognition, CheB recognizes methylated Glu residues to hydrolyze them, whereas CheR recognizes unmethylated Glu residues. Consistent with this consideration, *E. coli* CheB does not have a positively charged cluster in the primary sequence. Thus, it is intriguing to compare the mechanisms of receptor recognition of CheB with those of CheR.

Acknowledgments—We thank Drs. J. Beckwith and J. S. Parkinson for providing plasmids and bacterial strains. We acknowledge the following genome sequencing centers (and their funding agencies) for providing access to incomplete genome data: the Sanger Centre (Beowulf Genomics), the Joint Genome Institute (United States Department of Energy), the Institute for Genome Research (United States Department of Energy), and the University of Oklahoma (National Science Foundation).

REFERENCES

1. Manson, M. D. (1992) *Adv. Microbial. Physiol.* **33,** 277–346
2. Parkinson, J. S. (1993) *Cell* **73,** 857–871
3. Blair, D. F. (1995) *Annu. Rev. Microbiol.* **49,** 489–522
4. Stock, J. B., and Surette, M. G. (1996) in *Escherichia coli* and *Salmonella typhimurium*: *Cellular and Molecular Biology* (Neidhardt, F. C., Curtiss, R., III, Ingram, J. L., Lin, E. C. C., Low, K. B., Magasanik, B., Reznikoff, W. S., Riley, M., Schaechter, M., and Umbarger, H. E., eds) pp. 1103–1129, 2nd Ed., American Society for Microbiology, Washington, D. C.
5. Falke, J. J., Bass, R. B., Butler, S. L., Chervitz, S. A., and Danielson, M. A. (1997) *Annu. Rev. Cell Dev. Biol.* **13,** 457–512
6. Armitage, J. P. (1999) *Adv. Microb. Physiol.* **41,** 229–289
7. Bass, R. B., and Falke, J. J. (1999) *Structure* **7,** 829–840
8. Kim, K. K., Yokota, H., and Kim, S.-H. (1999) *Nature* **400,** 787–792
9. Wu, J., Li, J., Li, G., Long, D. G., and Weis, R. M. (1996) *Biochemistry* **35,** 4984–4993
10. Okumura, H., Nishiyama, S., Sasaki, A., Homma, M., and Kawagishi, I. (1998) *J. Bacteriol.* **180,** 1862–1868
11. Djordjevic, S., and Stock, A. M. (1998) *Nat. Struct. Biol.* **5,** 446–450
12. Shiomi, D., Okumura, H., Homma, M., and Kawagishi, I. (2000) *Mol. Microbiol.* **36,** 132–140
13. Djordjevic, S., and Stock, A. M. (1997) *Structure* **5,** 545–558
14. Maddock, J. R., and Shapiro, L. (1993) *Science* **259,** 1717–1723
15. Lybarger, S. R., and Maddock, J. R. (1999) *J. Bacteriol.* **181,** 5527–5529
16. Lybarger, S. R., and Maddock, J. R. (2000) *Proc. Natl. Acad. Sci. U. S. A.* **97,** 8057–8062
17. Skidmore, J. M., Ellefson, D. D., McNamara, B. P., Couto, M. M., Wolfe, A. J., and Maddock, J. R. (2000) *J. Bacteriol.* **182,** 967–973
18. Sourjik, V., and Berg, H. C. (2000) *Mol. Microbiol.* **37,** 740–751
19. Li, J., Li, G., and Weis, R. M. (1997) *Biochemistry* **36,** 11851–11857
20. Le Moual, H., and Koshland, D. E., Jr. (1997) *Biochemistry* **36,** 13441–13448
21. Feng, X., Lilly, A. A., and Hazelbauer, G. L. (1999) *J. Bacteriol.* **181,** 3164–3171
22. Subbaramaiah, K., Charles, H., and Simms, S. A. (1991) *J. Biol. Chem.* **266,** 19023–19027
23. Altschul, S. F., Madden, T. L., Schaffer, A. A., Zhang, J., Zhang, Z., Miller, W., and Lipman, D. J. (1997) *Nucleic Acids Res.* **25,** 3389–3402
24. Schultz, J., Milpetz, F., Bork, P., and Ponting, C. P. (1998) *Proc. Natl. Acad. Sci. U. S. A.* **95,** 5857–5864
25. Bateman, A., Birney, E., Durbin, R., Eddy, S. R., Howe, K. L., and Sonnhammer, E. L. (2000) *Nucleic Acids Res.* **28,** 263–266
26. Thompson, J. D., Gibson, T. J., Plewniak, F., Jeanmougin, F., and Higgins, D. G. (1997) *Nucleic Acids Res.* **25,** 4876–4882
27. Guex, N., and Peitsch, M. C. (1997) *Electrophoresis* **18,** 2714–2723
28. Parkinson, J. S., and Houts, S. E. (1982) *J. Bacteriol.* **171,** 6271–6278
29. Ames, P., Yu, Y. A., and Parkinson, J. S. (1996) *Mol. Microbiol.* **19,** 737–746
30. Wolfe, A. J., Conley, M. P., Kramer, T. J., and Berg, H. C. (1987) *J. Bacteriol.* **169,** 1878–1885
31. Ames, P., Studdert, C. A., Reiser, R. H., and Parkinson, J. S. (2002) *Proc. Natl. Acad. Sci. U. S. A.* **99,** 7060–7065
32. Guzman, L. M., Belin, D., Carson, M. J., and Beckwith, J. (1995) *J. Bacteriol.* **177,** 4121–4130
33. Bartolomé, B., Jubete, Y., Martinez, E., and Cruz, F. D. (1991) *Gene* (*Amst.*) **102,** 75–78
34. Landt, O., Grunert, H. P., and Hahn, U. (1990) *Gene* (*Amst.*) **96,** 125–128
35. Deleted in proof
36. Deleted in proof
37. Deleted in proof
38. Iwama, T., Homma, M., and Kawagishi, I. (1997) *J. Biol. Chem.* **272,** 13810–13815
39. Sogaard-Andersen, L., and Kaiser, D. (1996) *Proc. Natl. Acad. Sci. U. S. A.* **93,** 2675–2679
40. Lamb, J. R., Tuqendreich, S., and Hieter, P. (1995) *Trends Biochem. Sci.* **20,** 257–259
41. Das, A. K., Cohen, P. W., and Barford, D. (1998) *EMBO J.* **17,** 1192–1199
42. Taylor, B. L., and Zhulin, I. B. (1999) *Microbiol. Mol. Biol. Rev.* **63,** 479–506
43. Liu, J. D., and Parkinson, J. S. (1989) *Proc. Natl. Acad. Sci. U. S. A.* **86,** 8703–8707
44. Malone, T., Blumenthal, R. M., and Cheng, X. (1995) *J. Mol. Biol.* **253,** 618–632
45. Subbaramaiah, K., and Simms, S. A. (1992) *J. Biol. Chem.* **267,** 8636–8642
46. Kehry, M. R., Engstrom, P., Dahlquist, F. W., and Hazelbauer, G. L. (1983) *J. Biol. Chem.* **258,** 5050–5055
47. Simms, S. A., Stock, A. M., and Stock, J. B. (1987) *J. Biol. Chem.* **262,** 8537–8543
48. Yamamoto, K., Macnab, R. M., and Imae, Y. (1990) *J. Bacteriol.* **172,** 383–388
49. Barnakov, A. N., Barnakov, L. A., and Hazelbauer, G. L. (1999) *Proc. Natl. Acad. Sci. U. S. A.* **96,** 10667–10672
50. Barnakov, A. N., Barnakova, L. A., and Hazelbauer, G. L. (2001) *J. Biol. Chem.* **276,** 32984–32989